

GLASS TRANSITION FOR A HARD SPHERE MODEL FLUID FROM THE REPLICA ORNSTEIN-ZERNIKE APPROACH WITH HYPERNETTED CHAIN CLOSURE

O. Pizio^a, Yu. Duda^b, L. Pusztai^c, S. Sokolowski^d

^a *Universidad Autonoma Metropolitana, Iztapalapa, Mexico, D.F.*

^b *Programa de Ingenieria Molecular, Instituto Mexicano de Petroleo, 07730 Mexico, D.F.*

^c *Research Institute for Solid State Physics and Optics,
Hungarian Academy of Sciences, H-1525 Budapest, P.O. Box 49, Hungary*

^d *Department for the Modelling of Physico-Chemical Processes,
Maria Curie-Sklodowska University, Lublin 20031, Poland*

(Received 3 2009 .)

We review briefly the approach of Parisi and co-workers comprising replica Ornstein-Zernike integral equations with hypernetted chain closure to describe the glass transition for the model fluid of hard spheres. However, the original elements of the present communication are in the application of the expression for the fluid chemical potential in the replicated form and in the calculations of the isothermal compressibility. These tools permit us to characterize perfectly well the transition into glass phase without resorting to the explicit evaluation of the effective potential.

Keywords: integral equations, glass phase, chemical potential, hypernetted chain approximation

PACS: 74.72 Jt, 74.60 Ec

I. Brief review of the methodology

In the present work, we would like to investigate the glass transition in the one-component model fluid of hard spheres. The method has been developed quite recently by Parisi and coworkers [1, 2] but has not received much attention so far. Therefore, we feel appropriate to reconsider briefly the basic physical arguments and key ingredients of the approach for the sake of convenience of the reader. However, a comprehensive explanation of the method can be consulted in the original publications. In the specific model under consideration the only control parameter is the fluid density. However, for the sake of better understanding and having in mind other possible applications we present first the arguments in terms of fluid temperature rather than the density of particles. Consider a system that undergoes cooling from the liquid phase. At a certain temperature T_g , it falls out of equilibrium and remains stuck in a certain region of the configuration space. This situation is common at glass transition when the liquid stops flowing. Specifically, the large scale motion of particles is frozen while the small scale motion is still present (e.g. vibrations of atoms), these latter degrees of freedom still can equilibrate at temperatures below T_g . At such conditions, it is appropriate to restrict the measure in configuration space to the vicinity of a certain configuration y that is reached when the system crosses temperature T_g . In order to describe similarity or distance among different configurations, Parisi et al. [1, 2] have introduced a quantitative measure $q(x, y)$. Here and above the notation for the configuration of the system

of N particles is as common $x = (x_1, x_2, \dots, x_N)$. Moreover, let us mention that the system is encountered in the volume V and introduce notation for the interaction potential between particles as $u_{ff}(x_i - x_j)$. The similarity or co-distance between configurations will be called the overlap according to the original terminology. Similar configurations must correspond to high values of the overlap while very different configurations must correspond to very low values of the overlap q . Then the appropriate definition is

$$q(x, y) = \frac{1}{N} \sum_{i,j} w(|x_i - y_j|) \quad (1)$$

where the function $w(r)$ is chosen equal to 1 for small distances, $r < a\sigma$, and close to zero for $r > a\sigma$, where σ is the diameter of particles and a is a constant less than unity. In other words, couples of particles belonging to two configurations and located at small distances will contribute positively into q . One just needs to remember that high overlap means small distance between configurations. An initial ingredient of the theory is a restricted Boltzmann-Gibbs distribution function

$$P(x|y) = \frac{1}{Z(\beta, y)} \exp[-\beta H(x)] \delta(q(x, y) - q) \quad (2)$$

where $\beta = 1/k_B T$ is the inverse temperature and the normalizing partition function $Z(\beta, y)$ is the result of integration of the numerator of Eq.(2) over all configurations x . It is worth to comment that the configuration y is supposed to be a typical configuration of the system at T_g with respect to the Boltzmann-Gibbs probability distribution function. On the other hand, the value for

the parameter q in Eq.(2) is formally arbitrary. The system at certain temperature T will tend to adjust itself and select natural "distance" from the chosen configuration y , according to the free energy minimization. In some sense, the role of a configuration y is analogous to the one of quenched variables in the systems with structural disorder. Finally, it is necessary to make comment on the choice of T_g involved in the deliberations above. There is no any *a priori* criterion to use straightforwardly in this aspect. Actually, it is a quantity dependent on the cooling rate in the experiments. Therefore, it is natural to think off T_g as the temperature of the configuration y , this temperature will be called T' below. Thus, the probability to find y can be written as proportional to $\exp(-\beta' H(y))/Z(\beta')$. The key element of the theory of Parisi et al. [1, 2] is the so-called effective potential or in other words the free energy associated with the introduced Boltzmann-Gibbs distribution function,

$$V(q, \beta, \beta') = -\frac{T}{N} \frac{1}{Z(\beta)} \int dy \exp(-\beta' H(y)) * \ln \int dx \exp(-\beta H(x)) \delta(q(x, y) - q). \quad (3)$$

What is written here is in fact the average of the free energy associated with the distribution function given by Eq.(2) over realizations of the "self-generated disorder", the term frequently used in the theory of structural glasses. Equivalently, one can use the function $F(\varepsilon, \beta, \beta')$,

$$F(\varepsilon, \beta, \beta') = -\frac{T}{N} \frac{1}{Z(\beta)} \int dy \exp(-\beta' H(y)) * \ln \int dx \exp(-\beta[H(x) - \varepsilon q(x, y)]), \quad (4)$$

where ε is the Langrange multiplier, such that

$$V(q, \beta, \beta') = \min[F(\varepsilon, \beta, \beta') + \varepsilon q], \quad (5)$$

where c_{ab} are the direct correlation functions. In this equation above we have modified notations for the sake of compactness. Namely, $\beta' = \beta_0$, $\beta = \beta_a = \beta_b$ for all replicas distinct from the one numbered by zero. The correlation functions and the direct correlation functions satisfy the replicated Ornstein-Zernike equations, see e.g. [4]. The matrix with elements g_{ab} is parametrized implying replica symmetric structure: $g_{ab} = g_{00}$ for $a = b = 0$; $g_{ab} = g_{10}$ for $a = 0, b > 0$ or $b = 0, a > 0$.

where the minimum is taken with respect to ε . The expressions above for $V(q, \beta, \beta')$ and/or $F(\varepsilon, \beta, \beta')$ can be evaluated by using replica trick as common. The problem reduces to the calculation of thermodynamics of the system composed of $s+1$ replicas, actually the configuration y plays role of the replica with the index 0. It is a privileged component in the sense that the interaction between 0 replica and others is

$$N\varepsilon \sum_{a=1}^s = \varepsilon \sum_{a=1}^s \sum_{i,j}^N w(x_i^0 - x_j^a). \quad (6)$$

Note that we have changed notation and use here x^0 for the distinguished replica. In order to proceed further with the calculation of the free energy $F(\varepsilon, \beta, \beta')$, one can apply the hypernetted chain approximation that yield,

$$-\beta F_{HNC} = \frac{1}{2} \int d^3x \sum_{a,b=0}^s \rho_a \rho_b g_{ab}(x) [\ln g_{ab} - 1 + \beta_a u(x) \delta_{ab}] + \beta \varepsilon \sum_{a=1}^s \rho_0 \rho_a g_{0a}(x) w(x) + Tr[L(\rho h)], \quad (7)$$

where it is worth to recall that $u(x)$ is the interaction potential between particles. The free energy is given in terms of the pair distribution functions with subindices corresponding to replicas,

$$\rho_a \rho_b g_{ab}(x, y) + \rho_a \delta_{ab} \delta(x - y) = \sum_{i,j} \delta(x_i^a - x) \delta(x_j^b - y), \quad (8)$$

and $h_{ab} = g_{ab} - 1$ is the correlation function. The last term in Eq.(7) is the following abbreviation $L(f) = f - f^2/2 - \ln(1 + f)$. The trace over L concerns replica indexes and real space[1, 2]. The expression for the pair distribution functions in the HNC approximation can be obtained by taking the functional derivative of the free energy, see e.g. [3],

$$g_{ab}(r) = \exp(-\beta_a u(r) \delta_{ab} + [\delta_{0a}(1 - \delta_{0b})\beta_b + \delta_{0b}(1 - \delta_{0a})\beta_a] \varepsilon w(r) + h_{ab}(r) - c_{ab}(r)), \quad (9)$$

Next, $g_{ab} = g_{ab}^*$ if a and b are different then zero. These starred elements are $g_{ab}^* = g_{11}$ if $a = b$ and $g_{ab}^* = g_{12}$ if a and b do not coincide. This choice of the structure of the matrix with elements g_{ab} is similar to the structure applied by Given and Stell [5-7] for the description of partly quenched disordered systems. Technical aspects of the final stage of the theory can be resumed as follows. The principal task of the approach is to solve the replicated Ornstein-Zernike (ROZ) integral equations,

$$h_{00}(r_{12}) - c_{00}(r_{12}) = \rho_0 \int d\mathbf{r}_3 c_{00}(r_{13}) h_{00}(r_{32}) + \rho_1 \int d\mathbf{r}_3 c_{01}(r_{13}) h_{10}(r_{32}), \quad (10)$$

$$\begin{aligned}
 h_{10}(r_{12}) - c_{10}(r_{12}) &= \rho_0 \int d\mathbf{r}_3 c_{10}(r_{13}) h_{00}(r_{32}) + \rho_1 \int d\mathbf{r}_3 [c_{11}(r_{13}) \\
 &\quad + (s-1)c_{12}(r_{13})] h_{10}(r_{32}),
 \end{aligned} \tag{11}$$

$$\begin{aligned}
 h_{11}(r_{12}) - c_{11}(r_{12}) &= \rho_0 \int d\mathbf{r}_3 c_{10}(r_{13}) h_{10}(r_{32}) + \rho_1 \int d\mathbf{r}_3 c_{11}(r_{13}) h_{11}(r_{32}) \\
 &\quad + (s-1)\rho_1 \int d\mathbf{r}_3 c_{12}(r_{13}) h_{12}(r_{32}),
 \end{aligned} \tag{12}$$

$$\begin{aligned}
 h_{12}(r_{12}) - c_{12}(r_{12}) &= \rho_0 \int d\mathbf{r}_3 c_{10}(r_{13}) h_{10}(r_{32}) + \rho_1 \int d\mathbf{r}_3 c_{11}(r_{13}) h_{12}(r_{32}) \\
 &\quad + \rho_1 \int d\mathbf{r}_3 c_{12}(r_{13}) h_{11}(r_{32}) + (s-2)\rho_1 \int d\mathbf{r}_3 c_{12}(r_{13}) h_{12}(r_{32}),
 \end{aligned} \tag{13}$$

where $s+1$ is the number of replicas of the system as we have mentioned already. The limit $s=0$ is taken before the solution of Eqs.(10)–(13). The ROZ equations are supplemented by the HNC closure which can be written in the simpler form comparing to Eq.(9),

$$1 + h_{ij}(r) = \exp[-\beta u_{ij}(r)] \exp[h_{ij}(r) - c_{ij}(r)], \tag{14}$$

where i, j take values 0,1 and 2. There are four unknown functions according to the equations above, namely 00, 10, 11 and 12. Remember that $u_{12} = 0$, because particles belonging to different replicas do not interact. We would like to recall here that the model in question is solely density dependent, in addition we restrict ourselves to the case $\beta = \beta'$ similarly to the analysis provided in [1, 2]. Moreover,

$$u_{00}(r) = u_{11}(r) = u_{ff}(r), \tag{15}$$

$$u_{10}(r) = u_{01}(r) = \varepsilon w(r)$$

where $w(r)$ is taken similar to the original developments[1, 2] in the form

$$w(r) = 1, \quad r < 0.3\sigma_f, \tag{16}$$

$$w(r) = 0, \quad r > 0.3\sigma_f.$$

The energetic parameter $\varepsilon^* = \varepsilon/k_B T$ describes coupling (either attraction or repulsion dependent on the sign of ε) between the "reference" configuration of the system chosen as replica with number 0 and configurations corresponding to other replicas. The distinguished ($s=0$) and all other replicas are at the same density $\rho_0 = \rho_1 = \rho$. Without loss of generality the diameter of particles is taken as the length unit, $\sigma_f = 1$. The overlap

constant q is the function of coupling and is determined through the distribution function $g_{10}(r)$ as follows, cf. Eq.(6),

$$q(\varepsilon) = 4\pi\rho \int_0^\infty dr r^2 g_{10}(r) w(r). \tag{17}$$

The glassy behavior of the system is associated with nonconvexity of the effective potential $V(q)$,

$$V(q) = \int_d^q dq' \varepsilon(q') \tag{18}$$

where the lower limit of integration, d , is a constant chosen for convenience of calculations. The nonconvexity of $V(q)$ in turn is related to the existence of multiple solutions of the function $q(\varepsilon)$ at vanishing and zero coupling $\varepsilon \rightarrow 0$. In the fluid phase $q(\varepsilon)$ is a single valued function, the effective potential $V(q)$ has minimum at $\rho \int dx w(x)$ corresponding to the absence of any structure of the function $g_{10}(x)$ or in other words this function equals unity for all values of its argument. A strong coupling ε leads to the attraction of a system towards the reference configuration and forces the function g_{10} to acquire certain structure. Similar trends of behavior are expected for the function g_{12} . When the system approaches glass transition conditions, a solution of the ROZ/HNC will exist in which both functions $g_{10}(r)$ and $g_{12}(r)$ will have very pronounced structure even at zero coupling $\varepsilon = 0$. All this discussion actually is borrowed from [1, 2] to make things clearer for the reader.

On the other hand, we will show just now that important conclusions about glass transition for the model in question can be reached without resorting to the explicit calculation of the effective potential. In order to elucidate the glass transition we apply the expression for the chemical potential of the replicated system in the ROZ/HNC approximation [8],

$$\begin{aligned} \beta\mu_1 = & -\rho_0 \int d\mathbf{r} c_{00}(r) - \rho_1 \int d\mathbf{r} [c_{11}(r) - c_{12}(r)] + \frac{1}{2}\rho_0 \int d\mathbf{r} h_{10}(r)(h_{10}(r) - c_{10}(r)) \\ & + \frac{1}{2}\rho_1 \int d\mathbf{r} h_{11}(r)(h_{11}(r) - c_{11}(r)) - \frac{1}{2}\rho_1 \int d\mathbf{r} h_{12}(r)(h_{12}(r) - c_{12}(r)) \end{aligned} \quad (19)$$

Moreover, one can obtain the isothermal compressibility via commonly used expression for the replicated OZ equations with HNC closure resulting from the compressibility route to thermodynamics,

$$\kappa^* = \rho_1 \beta^{-1} \kappa = \beta^{-1} \left(\frac{\partial \rho}{\partial P} \right) = [1 - \rho_1 \int \mathbf{r} (c_{11}(r) - c_{12}(r))]^{-1}. \quad (20)$$

II. Results and discussion

Let us proceed to the numerical results. The ROZ/HNC equation have been solved by iterations on a grid of 2^{12} points with the step $\delta r = 0.005$ and by applying standard fast Fourier-transform routine. Next, the distribution functions provide $q(\varepsilon)$, the chemical potential and compressibility.

In Fig. 1a we present the dependence of the overlap on the coupling parameter $q(\varepsilon^*)$ at different fluid densities. The limiting density at which the overlap remains continuous is $\rho \simeq 1.065$ or in terms of the packing fraction $\eta = \pi\rho/6$ is $\eta = 0.5576$. At higher densities we observe two branches of $q(\varepsilon^*)$ that exhibit hysteresis at positive values of ε^* . A discontinuity is observed for the first time at $\rho = 1.07$ or $\eta = 0.56$. Many authors reported and discussed observation of a glass transition in a hard sphere fluid at this value of density [9–11]. It is documented that at this density, the particles are confined to "cages" by their neighbors and the fluid dynamics separates into a fast rattling inside the cage and slow rearrangements of the cages. One example of the behavior of the chemical potential at density $\rho = 1.10$ is given in Fig. 1b. There are two branches of the chemical potential dependence on ε^* and they join together via jump discontinuities. Interesting changes on the dependence of the overlap on coupling occur at higher densities, Fig. 2a. Namely, at $\rho \simeq 1.17$ ($\eta = 0.6126$) the branch corresponding to a high overlap crosses the zero coupling point. At slightly lower density, however, the chemical potential curves exhibit hysteresis located at positive values of ε^* (cf. Fig. 2b). In Ref. [2] it has been discussed that at such density the metastable states have an infinite time life (a minimum of the effective potential develops), in contrast to lower densities. Only at density approximately equal to 1.17 two branches of

the chemical potential cross at $\varepsilon^* = 0$ demonstrating coexistence of two phases characterized by a different amount of overlap (Fig. 2c). This "critical" density (packing fraction) is in the range of densities estimated for the commonly called ideal glass transition or Kauzmann transition $\eta = 0.58 - 0.62$. However, at Kauzmann density the "configurational" entropy must vanish. In contrast, the ROZ/HNC approach in the Parisi et al. [1, 2] version provides small but definitely nonzero entropy at this density. At higher densities than $\rho = 1.17$ we again observe crossing of two branches of the chemical potential (Fig. 2d) and cannot establish upper limit of the application of the expression (19). However, if one employs some sort of Maxwell construction to the $q(\varepsilon^*)$ curves in Fig. 2a, it can be deduced that the "end point" must be at $\rho \simeq 1.19$. On the other hand, if one resorts to the calculation of the effective potential by using Eq. (18) and calculates the configurational entropy from the difference of two minima of the effective potential, similar value for limiting density can be found [1, 2]. At this density the configurational entropy vanishes. These data in fact demonstrate strength and failures of the ROZ/HNC approach involving concept of the effective potential.

Finally we would like to provide some comments about the behavior of the isothermal compressibility. A set of results concerning it is shown in Fig. 3. At low density ($\rho = 1.065$) the line of compressibility values does not exhibit discontinuities but has a maximum at certain value of ε^* corresponding to the highest derivative of the function $q(\varepsilon^*)$, cf. Fig. 1a. Interestingly, at a higher density, $\rho = 1.10$, we observe that at a certain coupling the compressibilities of systems characterized by a low and a high overlap can be equal (Fig. 3b). At even higher density, $\rho = 1.15$, the dependence of the isothermal compressibility on coupling strength ε^* exhibits hysteresis in the region of positive values for ε^* . Finally, at $\rho = 1.185$ (as well as at $\rho = 1.18$) the hysteresis involves the point of zero coupling strength, Fig. 3d. The coexisting phases (according to the chemical potential behavior cf. Fig. 2d) are characterized by different compressibilities. This observation is in accordance with the results for the pressure dependence on density around glass transition, cf. Fig. 4 of the recent work of Parisi and Zamponi [11].

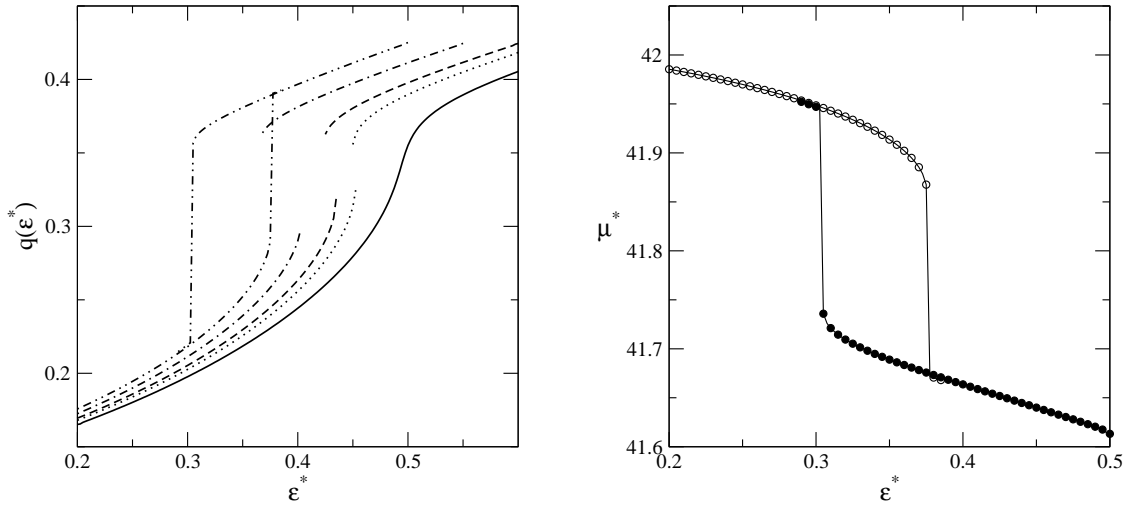


Fig. 1. Part a: The dependence of the overlap function on the coupling parameter $q(\varepsilon^*)$ at different fluid densities. The solid, dotted, short-dash, dash-dotted and dash - double dotted lines are for the fluid density $\rho = 1.065, 1.075, 1.08, 1.09$ and 1.10 , respectively. Part b: The dependence of the chemical potential on the coupling parameter $\mu^*(\varepsilon^*)$ at $\rho = 1.10$ ($\mu^* = \mu_1/k_B T$) The hollow and filled circles correspond to the branches of increasing and decreasing q values, respectively

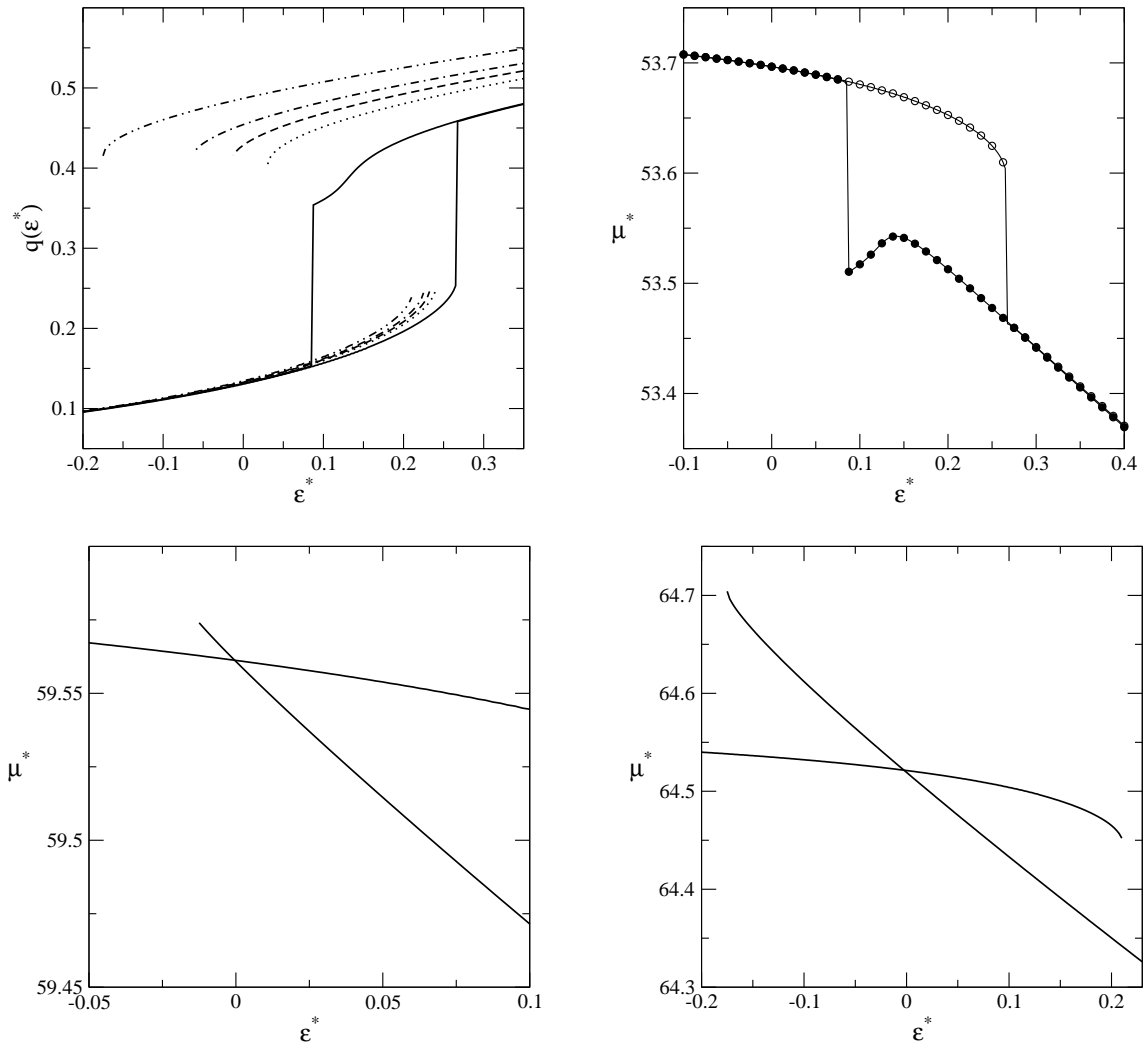


Fig. 2. Part a: The dependence of the overlap function on the coupling parameter $q(\varepsilon^*)$ at different fluid densities. The solid, dotted, short-dash, dash-dotted and dash - double dotted lines are for the fluid density $\rho = 1.15, 1.165, 1.17, 1.175$ and 1.185 , respectively. Parts b, c and d: The dependence of the chemical potential on the coupling parameter $\mu^*(\varepsilon^*)$ at $\rho = 1.15$ (part b), $\rho = 1.17$ (part c) and $\rho = 1.185$ (part d)

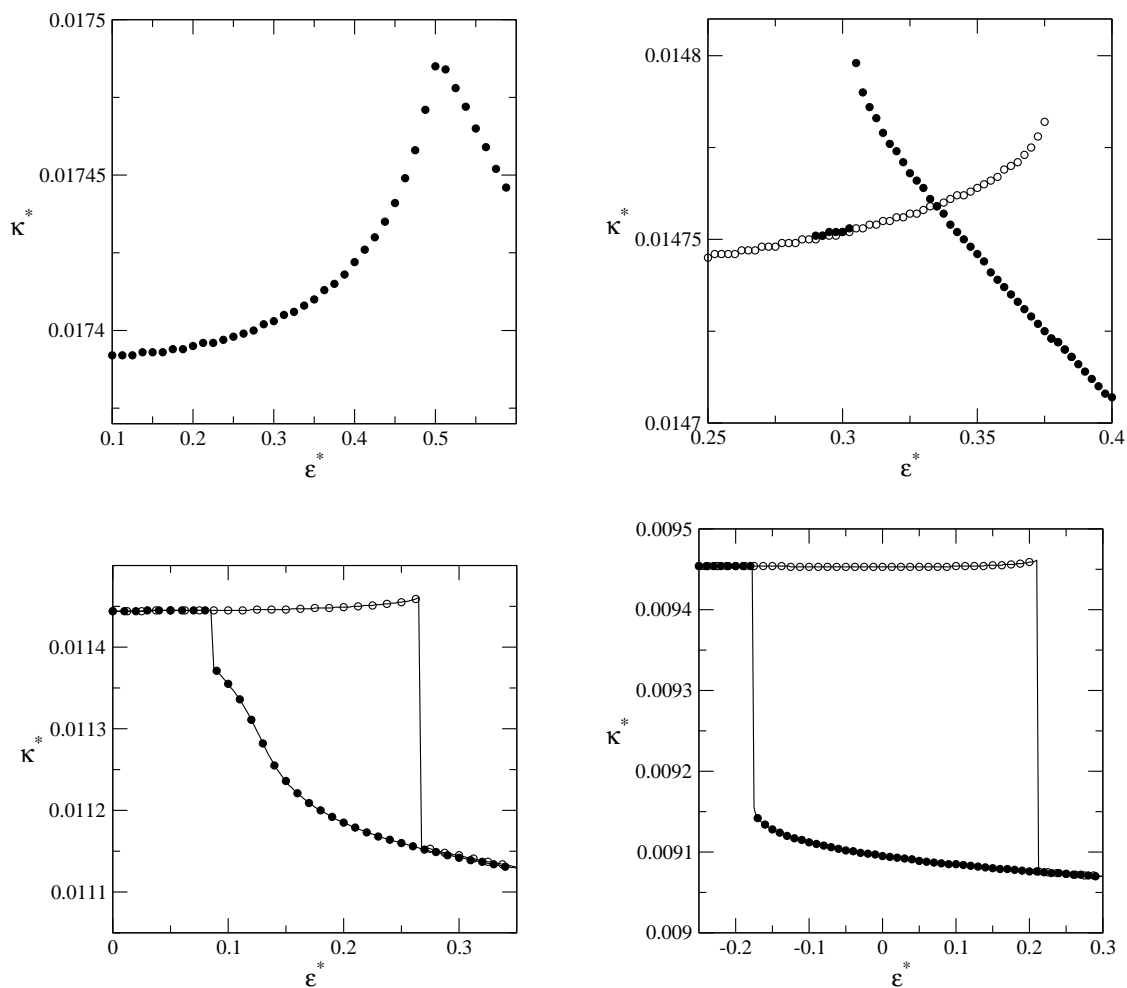


Fig. 3. The dependence of the isothermal compressibility on the coupling parameter, $\kappa^*(\varepsilon^*)$, at $\rho = 1.065$ (part a), $\rho = 1.10$ (part b), $\rho = 1.15$ (part c) and $\rho = 1.185$ (part d), respectively

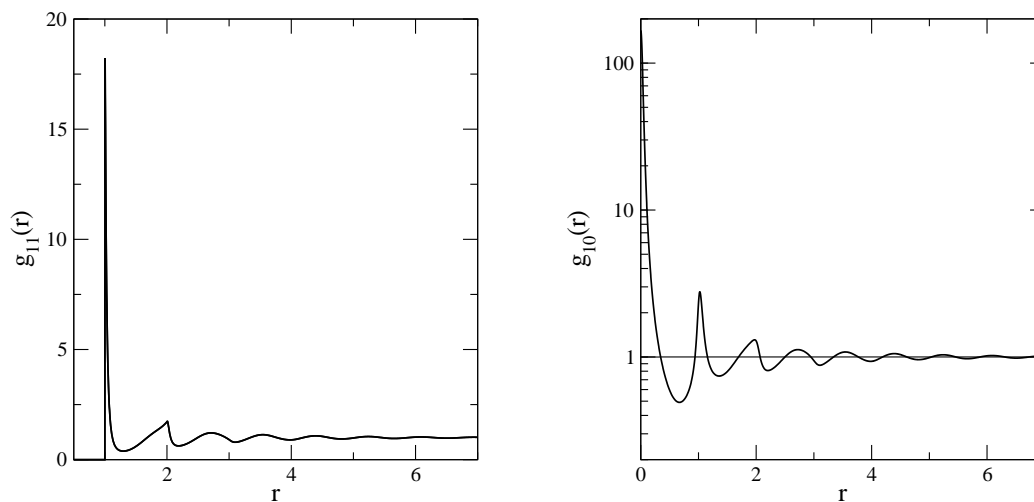


Fig. 4. The pair distribution function $g_{11}(r)$ (part a) and $g_{10}(r)$ (part b) at $\rho = 1.17$ at zero coupling $\varepsilon^* = 0$. The thin solid line in part b shows $g_{10}(r) \simeq 1.0$ on the branch of low q values at zero coupling $\varepsilon^* = 0$ whereas the thick solid line shows the same function at zero coupling on the branch of high q

We have already commented above on the expected changes of the distribution functions g_{10} and g_{12} during glass transition. In order to provide illustration, we present the distribution functions g_{11} and g_{10} in parts

a and b of Fig. 4. These functions are shown at the density $\rho = 1.17$ at zero coupling strength $\varepsilon^* = 0$. The function $g_{11}(r)$ is equal to $g_{00}(r)$ and is characterized by a very high and sharp peak at $r = 1^+$, one can see a very

weakly pronounced smooth shoulder around $r = 1.5$, this shoulder could be very pronounced if the system would undergo spontaneous crystallization (cf. Fig. 10 of Ref. [2]). Drastic changes are observed on the function $g_{10}(r)$ if one compares the curves corresponding to a low $q(\varepsilon^*)$ branch (thin line in Fig. 4b) of the overlap function with a high q branch (thick line in Fig. 4b) at zero coupling strength.

To conclude, we have carefully checked the results obtained previously in Refs. [1, 2] and performed our own more precise calculations of the distribution functions involved in the solution of the replicated Ornstein-Zernike equations with hypernetted chain closure. Moreover we have augmented findings concerning glass transition in the model fluid of hard spheres by considering chemical potential and isothermal compressibility. We have found two characteristic densities. One of them corresponds to the beginning of the jump

discontinuity on the dependence of the overlap function on coupling strength, this density coincides with previously reported data on glass transition. In addition we have found the value of density at which the branches of the chemical potential for low and high overlaps cross at zero coupling strength. At this coexistence the isothermal compressibility corresponding to two branches is different as expected at glass transition. Further research to describe thermodynamics of glass transition in this model fluid and related systems is necessary along lines provided in e.g. Ref. [11].

III. Acknowledgements

This project has been partially supported by the National University of Mexico under grant IN-223808-2. *O.P. is on sabbatical leave from Instituto de Quimica de la UNAM.

References

- [1] M. Cardenas, S. Franz, G. Parisi (1998) J. Phys. A: Math. Gen., **31**, L163.
 [2] M. Cardenas, S. Franz, G. Parisi (1999) J. Chem. Phys., **110**, 1726.
 [3] I.R. Yukhnovsky, M.F. Holovko, Statistical Theory of Classical Equilibrium Systems, Kiev, Naukova Dumka (1980), in Russian.
 [4] O. Pizio, Adsorption in Random Porous Media, in: Computational Methods in Surface and Colloid Science, (M. Borowko, Ed.) Marcel Dekker, New York, 2000.
 [5] J. A. Given and G. Stell (1994) Physica A, **209**, 405.
 [6] J.A. Given and G. Stell (1992) J. Chem. Phys., **97**, 4573.
 [7] J. A. Given (1995) J. Chem. Phys., **102**, 2934.
 [8] B. Hribar, V. Vlachy, O. Pizio (2002) Molec. Phys., **100**, 3093.
 [9] W. Gotze, L. Sjogren (1991) Phys. Rev. A, **43**, 5442.
 [10] W. van Meegen, S.M. Underwood (1993) Phys. Rev. Lett., **70**, 2766.
 [11] G. Parisi, F. Zamponi (2005) J. Chem. Phys., **123**, 144501.

ОПИС ПЕРЕХІД У ФАЗУ СКЛА В МОДЕЛІ ТВЕРДИХ КУЛЬОК МЕТОДОМ ІНТЕГРАЛЬНОГО РІВНЯННЯ ОРНШТЕЙНА-ЦЕРНІКЕ У ГІПЕРЛАНЦЮГОВОМУ НАБЛИЖЕННІ

О. Пізіо^a, Ю. Дуда^b, Л. Пуштай^c, С. Соколовський^d

^a Автономний університет Метрополітана,
Ітаралана, Мехіко, Д.Ф.

^b Програма молекулярної інженерії, Мексиканський Інститут нафти,
07730, Мехіко Д.В.

^c Дослідний інститут твердого тіла і оптики,
Угорська Академія Наук, H-1525, Будапешт
Поштова скринька 49, Угорщина

^d Відділ моделювання фізико-хімічних процесів,
Університет Марії Кюрі-Скłodовської,
Люблін 20031, Польща

Ми виконали огляд методу Парізі та співробітників, який включає репліковане інтегральне рівняння Орнштейна-Церніке у гіперланцюгованому наближенні до опису переходу у фазу скла в моделі твердих кульок. Оригінальні елементи роботи полягають у застосуванні виразу для хімічного потенціалу та ізотермічної стисливості. Застосовані методи дозволили описати перехід у фазу скла без застосування концепції ефективного потенціалу.

Ключові слова: Інтегральні рівняння, фаза скла, хімічний потенціал, гіперланцюгове наближення.

PACS: 74.72 Jt, 74.60 Ec